ChemPubSoc Europe

DOI: 10.1002/batt.201800042

BATTERIES & SUPERCAPS Communications

DRILL Interface Makes Ion Soft Landing Broadly Accessible for Energy Science and Applications

Grant E. Johnson,*[a] Venkateshkumar Prabhakaran,[a] Nigel D. Browning,[b] B. Layla Mehdi,[b] Julia Laskin,[c] Peter A. Kottke,[d] and Andrei G. Fedorov[d]

Polyoxometalates (POM) have been deposited onto carbon nanotube (CNT) electrodes using benchtop ion soft landing (SL) enabled by a vortex-confined electrohydrodynamic desolvation process. The device is based on the dry ion localization and locomotion (DRILL) mass spectrometry interface of Fedorov and co-workers. By adding electrospray emitters, heating the desolvation gas, and operating at high gas flow rates, it is possible to obtain stable ion currents up to −15 nA that are ideal for deposition. Coupled with ambient ion optics, this interface enables desolvated ions to be delivered to surfaces while excluding solvent and counterions. Electron microscopy of surfaces prepared using the device reveal discrete POM and no aggregation that degrades electrode performance. Characterization of POM-coated CNT electrodes in a supercapacitor showed an energy storage capacity similar to that achieved with SL in vacuum. For solutions that produce primarily a single ion by electrospray ionization, benchtop SL offers a simpler and less costly approach for surface modification with applications in catalysis, energy storage, and beyond.

Soft landing (SL) of ions onto surfaces is a versatile approach for precisely-controlled preparation of materials for applications and fundamental research in materials, physics, chemistry, and biology.[1–7] Recent reports have demonstrated the use of SL for preparation of well-defined model catalysts through deposition of mass-selected clusters, nanoparticles, and organometallics.[8–16] SL also has been used to deliver nanoparticles to tissue where they serve as an ionization enhancing matrix for mass spectrometry imaging.[17–18] Other applications of SL include purification and conformational enrichment of peptides and proteins,[19–21] chiral amplification of molecules,[22] and preparation of thin films.[23] SL of low kinetic energy ions for surface modification was first demonstrated by Cooks and co-workers.[24] Since this initial report advances have been made in ionization sources,[25,26] ion optics,[27] and mass filters[28] that allow deposition of a range of ions, simultaneous SL of multiple ions, and high flux ion deposition to prepare multilayer films.[29,30] Revealing the ongoing interest in these capabilities, vacuum-based electrospray deposition systems are available from companies such as MolecularSpray (http://www.molecularspray.co.uk/).

In an advancement, SL was transitioned out of vacuum and used to prepare surfaces containing ions of selected polarity at ambient conditions.[31] This simplified approach also has been employed to separate isomers from reactions of SL ions with surfaces that otherwise produce a distribution of isomeric products when reacted in solution.[32] In another application, ambient SL was used to deposit metal oxides onto surfaces for matrix assisted laser desorption ionization mass spectrometry (MALDI-MS) and in-situ enrichment of phosphopeptides.[33] Catalytic nanoparticles have been produced at ambient conditions through electro-corrosion of metals combined with electrospray ionization and deposition of the solvated cations.[34] In addition, it was shown that arrays of metallic nanostructures that provide surface enhanced Raman spectroscopy (SERS) enhancement factors of up to 10^9 may be prepared using ambient electrolytic spray deposition combined with a mask.[35] With these recent developments, SL offers solutions to surface modification problems across a wide range of research fields at both vacuum and ambient conditions. An important question, however, remains regarding whether or not simplified SL performed on the benchtop is capable of delivering discrete ions to surfaces in a way that prevents aggregation and maximizes the "active fraction" of the material.

In a recent publication, we reported preparation of model electrochemical capacitors (redox supercapacitors) with improved energy storage capacity and stability using SL of mass-selected POM ions in vacuum.[36] Through a combination of electrochemical techniques and electron microscopy it was shown that mass-selected molybdenum POM anions ($PMo_{12}O_{40}^{3-}$) SL onto carbon nanotube (CNT) electrodes without counterions or solvent attach to the electrode as discrete molecules. In contrast, the same species prepared by ambient electrospray deposition, where both counterions and solvent are present in solution droplets that reach the surface, were

[a] Dr. G. E. Johnson, Dr. V. Prabhakaran
Physical Sciences Division
Pacific Northwest National Laboratory
Richland, WA 99352 (USA)
E-mail: Grant.Johnson@pnnl.gov
[b] Prof. N. D. Browning, Dr. B. L. Mehdi
School of Engineering
Department of Mechanical & Aerospace Engineering
University of Liverpool
Liverpool, L69 3GQ, (UK)
[c] Prof. J. Laskin
Department of Chemistry
Purdue University
West Lafayette, IN 47907 (USA)
[d] Dr. P. A. Kottke, Prof. A. G. Fedorov
School of Mechanical Engineering
Georgia Institute of Technology
Atlanta, GA 30332 (USA)
Supporting Information and the ORCID identification number(s) for the author(s) of this article can be found under:
https://doi.org/10.1002/batt.201800042

found to form larger aggregates resulting in inferior electrode performance. The superior performance of the capacitors assembled from SL electrodes prepared in vacuum was attributed to the uniform distribution of redox-active ions and elimination of redox-inactive counter ions and solvent from the interface. These previous observations motivated the current study where the objective was to deposit discrete POM anions onto electrodes without any solvent or cations at benchtop conditions. This development in benchtop deposition, inspired by previous research on ambient SL,[31] provides a pathway for scaling up the technique for a broader range of applications. Higher deposition rates will enable rational design of functional surfaces with chemical control over the distribution of ions along with elimination of non-active species that is needed to achieve superior device performance by preventing the process of aggregate formation. Further advantages of benchtop SL include its reduced cost and easier operation which will make SL more accessible to the broad scientific community.

The modified DRILL interface used to deposit POM anions at benchtop conditions is shown in Figure 1. Similar to the

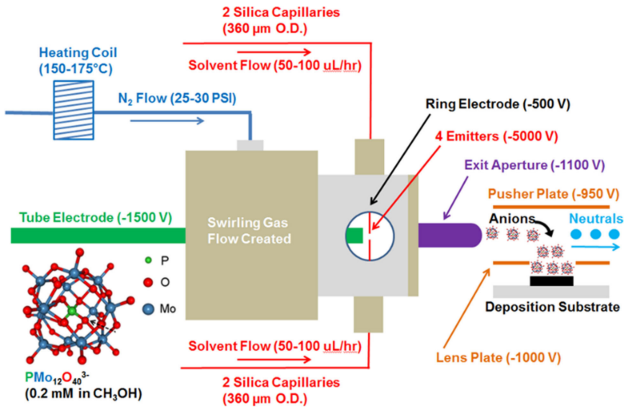

Figure 1. Dry ion localization and locomotion (DRILL) interface and accompanying ion optics used for benchtop ion soft landing.

original device,[37] the modified DRILL interface is cylindrical and consists mainly of polyether ether ketone (PEEK) and aluminum. The drying gas (N_2, 30 PSI) is directed through multiple specially-designed apertures in the PEEK cylinder that cause the flow to acquire a vortex-like trajectory. An important update to the DRILL system for benchtop SL is the incorporation of a heated drying gas, which aids efficient desolvation of ions in solution for a greater flow rate of multiple electrospray emitters. The vortical flow of heated gas ($T = 175\,^{\circ}C$) generated in the PEEK swirl generator is transmitted through an adjustable converging aperture into the smaller diameter aluminum cylinder where desolvation of charged solvent droplets generated by electrospray ionization occurs. Three electrodes are present in the desolvation region (Figure 1) including the long back tube electrode, short exit aperture tube, and the outer shell electrode. Commercial PEEK fittings (Upchurch) are used to equip the desolvation region with a gas-tight seal while allowing the position of the back and front electrodes to be

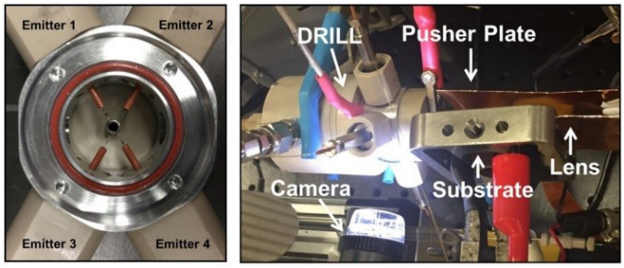

Figure 2. Photograph of the modified DRILL interface incorporating four electrospray emitters in the desolvation region of the device (left). Photograph of the benchtop ion soft landing equipment with the DRILL interface (right). The aluminum cylinder in the left image has a diameter of 3.5 cm.

adjusted to optimize ion current. Two quartz windows are mounted on the aluminum cylinder, which provide optical access for a digital camera (Figure 2, right). The camera aids alignment of each electrospray emitter and allows the operator to observe the effect of changes in source parameters (spray voltage, solution flow rate) on the electrospray process in real time. All interfaces with the atmosphere are sealed with gas-tight O-rings. Ensuring a complete seal of the device during operation is critical to achieving sufficiently intense and stable ion currents for efficient deposition.

Unlike the original single-emitter DRILL interface, which was configured to maximize ion signal-to-noise ratios for analytical applications, the modified device shown in Figures 1 and 2 is designed to maximize total ion current and has a total of four electrospray emitters located radially around the circumference of the aluminum desolvation region (Figure 2, left). The four emitters extend inward from the ring electrode and are fixed at an equal distance from the back-tube electrode (Figure 1, green). The position of the back-tube electrode with respect to the emitters was determined to have a substantial effect on the ion current and to be optimal at a position 5–8 mm behind the emitters. The back-tube electrode provides a repulsive potential behind the region where charged droplets are formed. This provides the charged droplets with an initial velocity toward the gas vortex region where desolvation occurs. Fused silica capillaries (360 µm OD/100 µm ID) were used as electrospray emitters to prevent clogging of the lines which became an issue for narrower ID capillaries at long deposition times (>4 hrs). During deposition of POM anions, the four emitters were operated at −7 kV which is higher than the typical ESI voltage used for analytical MS. The higher voltage ensured maximum ion current from the four larger ID capillaries located in close proximity. The optimum potentials for POM deposition for each of the electrodes are provided in Figure 1. Generally, at the higher gas flow rates used for benchtop SL, the most sensitive electrode setting was the exit aperture tube. The influence of the back-tube electrode, which has a pronounced effect on the ion current at lower gas flow rates used for analytical applications, was dampened at the higher gas flow rates. This was also the case for the ring electrode, the potential of which did not exert a strong influence on the ion current at higher gas flow rates. After leaving the desolvation region through the exit aperture the ions encounter a parallel pusher plate biased

at around −950 V which directs the beam of desolvated POM anions toward the grounded deposition substrate. This off-axis geometry ensures that no counterions or neutral molecules reach the substrate. It also prevents the surface from being continually bombarded by heated gas flow throughout the deposition. An initial configuration of the deposition apparatus with only the pusher plate resulted in depositions that were poorly focused and spread out over a large area. By introducing a parallel copper lens plate with a 1 cm diameter circular orifice biased to −1 kV between the pusher plate and the surface, it was possible to focus the ions at ambient conditions resulting in even and reproducible coverages of POM on the substrates.

Recently, we demonstrated that SL of discrete POM anions onto CNT electrodes without any contaminants resulting from solvent and counterions produced a model supercapacitor device with superior capacity and durability toward repeated charge-discharge cycling.[36] Using high-resolution STEM imaging, the enhanced performance of these electrodes was attributed to the elimination of POM aggregation. Aggregation results in a fraction of material that is not accessible for electron transfer at the electrode interface. To determine whether the benchtop DRILL interface can prepare electrodes similar to those SL in vacuum, it is necessary to compare supported POMs prepared using both techniques. To examine the uniformity of dispersion of the SL $PMo_{12}O_{40}^{3-}$ anions, we deposited them onto graphene-coated TEM grids using both the vacuum-based and benchtop SL approach and characterized them using HAADF-STEM. The images of benchtop and vacuum SL POM are shown in Figure 3. In the images, individual POM may be observed for both deposition methods confirming that discrete cluster ions may be prepared using benchtop SL with the modified DRILL interface. These images are strikingly different to those obtained previously for direct electrospray deposition (ESD) of POM onto CNT electrodes where larger aggregates were formed due to the presence of counterions and solvent at the interface.[36] However, a more subtle difference between the surfaces prepared in vacuum and on the benchtop may be seen in the longer-range structures adopted by POMs on the graphene TEM grid (Figure 3a and 3c). Mass-selected SL of POM in vacuum forms open and web-like extended structures with the POMs constituting the strands of the webs in close proximity. Large open spaces devoid of POM are also present for the POM prepared by SL in vacuum. In comparison, POM SL with DRILL on the benchtop do not show this web-like arrangement on the surface and instead form isolated islands of clusters with diameters of 25–35 nm, as shown in Figure 3c. These islands typically contained higher coverages of POM at the center and the coverage decreases closer to their outside edges. Therefore, when viewed at a larger scale there are differences in the extended structures formed by POM at different SL conditions. Inspection of the STEM images at higher magnification, however, reveals that while the intercluster distances may be different, the nature of the individual POMs at the graphene interface is similar for the two techniques. Specifically, POM SL in vacuum and on the benchtop with DRILL are distinguishable as discrete entities on the surface of the grid without formation of larger aggregates. As we will show next, this is the critical factor underlying the performance of the model supercapacitors assembled using both deposition techniques.

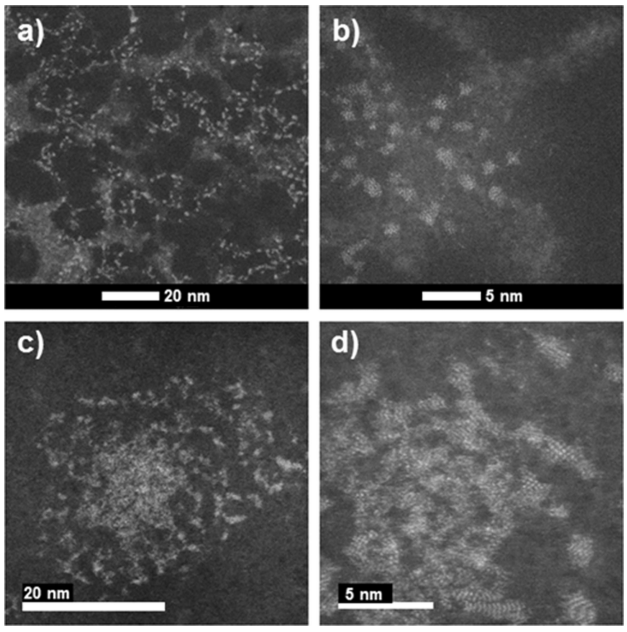

Figure 3. High-angle annular dark field scanning transmission electron micrographs of $PMo_{12}O_{40}^{3-}$ deposited onto graphene-coated TEM grids. HAADF-STEM images of mass selected POM anions soft landed in vacuum (a, b), images of POM anions deposited at benchtop conditions using the modified DRILL interface (c, d).

To test the performance of CNT electrodes modified with POM in a model supercapacitor device, electrodes with similar loading were prepared and assembled.[36] The cyclic voltammograms (CV), Galvanostatic charge-discharge (GCD) curves, and the estimated total specific capacitance of the model redox supercapacitors fabricated using benchtop and vacuum-based SL are shown in Figure 4. The rectangular CV and triangular GCD curves presented in Figure 4 (a & b) confirm the presence of ideal capacitive-like behavior without diffusion-limited and interfacial contact resistance. The CVs of the electrodes prepared by benchtop and vacuum-based SL showed higher capacitance compared to the pristine CNT. This is also the case for the GCD measurements where both SL techniques increased the performance of the POM-modified electrodes compared to the pristine CNT. The total specific capacitance of the pristine CNT, benchtop, and vacuum SL electrodes were calculated to be 125, 186, and 195 $A\,g^{-1}$, respectively.

The increase in the total specific capacitance of SL electrodes compared to pristine electrodes demonstrates the presence of additional Faradaic capacitance due to the multi-electron redox activity of $PMo_{12}O_{40}^{3-}$. This observation is in line with our previous reports on similar redox supercapacitors fabricated using vacuum-based SL. Additionally, the total specific capacitance of the vacuum SL electrodes is slightly higher (~4%) than that of the benchtop. This small difference in capacitance may be due to 2- anions that are present on the benchtop SL electrode whereas all of the mass-selected anions deposited in vacuum are 3-. The existence of comparable specific capaci-

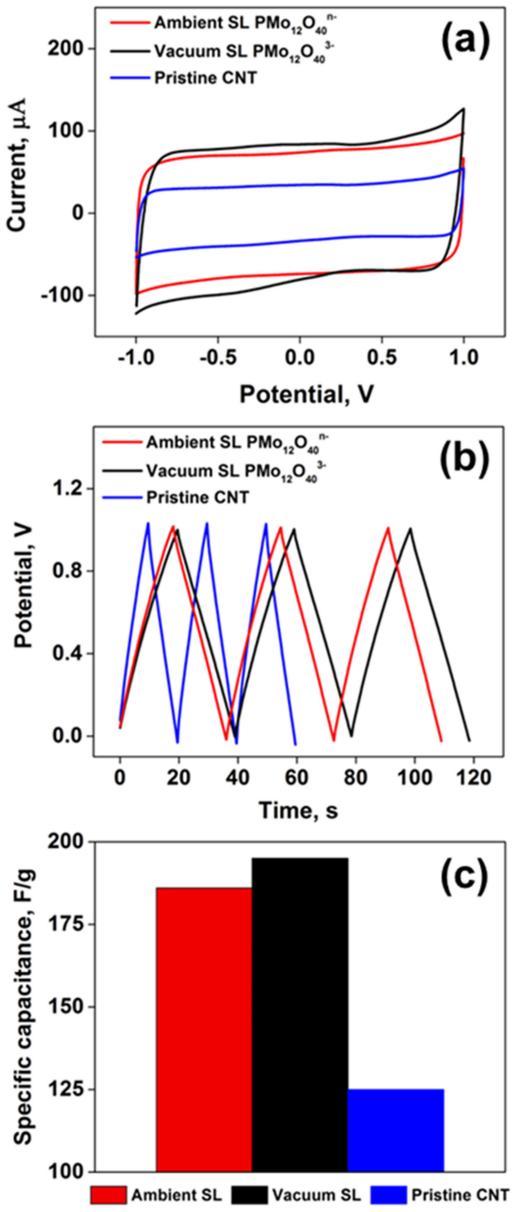

Figure 4. Electrochemical characterization of model supercapacitors fabricated with benchtop ion soft landing, vacuum-based soft landing of mass-selected ions and pristine carbon nanotube electrodes. a) Representative cyclic voltammograms, b) galvanostatic charge-discharge curves and c) total specific capacitance.

tance in benchtop SL electrodes and those prepared in vacuum is attributed to the complete elimination of strongly coordinating counter cations and solvent molecules and uniform distribution of $PMo_{12}O_{40}^{3-}$ anions on the CNT electrodes.

These findings represent a substantial breakthrough in material preparation as it is now possible, for solutions that create mainly one ion by electrospray ionization, to achieve nearly identical device performance using benchtop SL in a configuration that is less costly and far easier to operate than vacuum-based ion SL. The DRILL interface will make the SL approach to surface modification available to more of the scientific community. Complex solutions that produce a broad distribution of ions in the ionization process, however, will still require mass-selection and vacuum conditions to isolate an ion with predetermined composition for deposition.

Herein, we report the development of benchtop ion SL using a modified DRILL interface to deposit uniform distributions of electroactive ions onto technologically-relevant electrode substrates. This simpler approach avoids the complications resulting from contamination with counter ions and solvent and enables preparation of functional electrodes for energy storage (supercapacitors). Using multi-electron redox active $PMo_{12}O_{40}^{3-}$ as a model system, we compared the dispersion and functionality of deposited ions on identical CNT electrode surfaces prepared using benchtop and vacuum-based ion SL. HAADF-STEM images confirm that the distribution of $PMo_{12}O_{40}^{3-}$ anions produced on the surface using benchtop SL is comparable to that obtained in vacuum with mass-selection. Additionally, the model POM-based redox supercapacitor devices fabricated using benchtop and vacuum SL exhibit similar capacitance consistent with a comparable POM-electrode interaction. Our earlier studies established that SL of mass-selected ions in vacuum is useful to obtain a fundamental molecular-level understanding of functional interfaces where higher accuracy and precision in composition of the ions to be deposited is necessary. We believe that the benchtop SL technique introduced in this work will extend this research to larger scale device fabrication. This capability will help transform the knowledge obtained from fundamental studies of idealized surfaces to enable the rational design of functional interfaces for energy storage devices and other technologies where controlled surface modification is required.

Acknowledgements

The authors acknowledge support from the U.S. Department of Energy (DOE), Office of Science, Office of Basic Energy Sciences, Division of Chemical Sciences, Geosciences and Biosciences and Materials Science and Engineering, Synthesis and Processing Science. The research described herein was performed using EMSL, a DOE Office of Science User Facility sponsored by the Office of Biological and Environmental Research. PNNL is a multiprogram national laboratory operated for DOE by Battelle. P.A.K. was supported by the National Institute of General Medical Sciences of the National Institutes of Health under Award Number R01GM112662 (DRILL design and simulations). A.G.F. was supported by the U.S. Department of Energy (DOE), Office of Science, Basic Energy Sciences (BES), under Award #DE-SC0010729 (electrospray-based nanomaterial deposition).

Conflict of Interest

The authors declare no conflict of interest.

Keywords: deposition · electrochemistry · electron microscopy · energy storage · soft landing

[1] G. E. Johnson, D. Gunaratne, J. Laskin, *Mass Spectrom. Rev.* **2015**.
[2] J. Laskin, G. E. Johnson, V. Prabhakaran, *J. Phys. Chem. C* **2016**, *120*, 23305–23322.
[3] G. Verbeck, W. Hoffmann, B. Walton, *Analyst* **2012**, *137*, 4393–4407.
[4] S. Rauschenbach, M. Ternes, L. Harnau, K. Kern, *Annu. Rev. Anal. Chem.* **2016**, *9*, 473–498.
[5] J. Cyriac, T. Pradeep, H. Kang, R. Souda, R. G. Cooks, *Chem. Rev.* **2012**, *112*, 5356–5411.
[6] G. E. Johnson, Q. C. Hu, J. Laskin, *Ann. Rev. Anal. Chem.* **2011**, *4*, 83–104.
[7] V. Grill, J. Shen, C. Evans, R. G. Cooks, *Rev. Sci. Instrum.* **2001**, *72*, 3149–3179.
[8] S. Vajda, M. G. White, *ACS Catal.* **2015**, *5*, 7152–7176.
[9] E. C. Tyo, S. Vajda, *Nat. Nanotechnol.* **2015**, *10*, 577–588.
[10] A. S. Crampton, M. D. Rotzer, C. J. Ridge, F. F. Schweinberger, U. Heiz, B. Yoon, U. Landman, *Nat. Commun.* **2016**, *7*, 10389.
[11] V. Habibpour, M. Y. Song, Z. W. Wang, J. Cookson, C. M. Brown, P. T. Bishop, R. E. Palmer, *J. Phys. Chem. C* **2012**, *116*, 26295–26299.
[12] A. von Weber, S. L. Anderson, *Acc. Chem. Res.* **2016**, *49*, 2632–2639.
[13] P. Hernandez-Fernandez, F. Masini, D. N. McCarthy, C. E. Strebel, D. Friebel, D. Deiana, P. Malacrida, A. Nierhoff, A. Bodin, A. M. Wise, J. H. Nielsen, T. W. Hansen, A. Nilsson, I. E. L. Stephens, I. Chorkendorff, *Nat. Chem.* **2014**, *6*, 732–738.
[14] N. Bajales, S. Schmaus, T. Miyamashi, W. Wulfhekel, J. Wilhelm, M. Walz, M. Stendel, A. Bagrets, F. Evers, S. Ulas, B. Kern, A. Bottcher, M. M. Kappes, *J. Chem. Phys.* **2013**, *138*, 104703.
[15] X. Tang, D. Bumueller, A. Lim, J. Schneider, U. Heiz, G. Gantefor, D. H. Fairbrother, K. H. Bowen, *J. Phys. Chem. C* **2014**, *118*, 29278–29286.
[16] S. Bonanni, K. Ait-Mansour, W. Harbich, H. Brune, *J. Am. Chem. Soc.* **2014**, *136*, 8702–8707.
[17] B. L. Walton, G. F. Verbeck, *Anal. Chem.* **2014**, *86*, 8114–8120.
[18] L. Muller, K. Baldwin, D. C. Barbacci, S. N. Jackson, A. Roux, C. D. Balaban, B. E. Brinson, M. I. McCully, E. K. Lewis, J. A. Schultz, A. S. Woods, *J. Am. Soc. Mass Spectrom.* **2017**, *28*, 1716–1728.
[19] V. A. Mikhailov, T. H. Mize, J. L. P. Benesch, C. V. Robinson, *Anal. Chem.* **2014**, *86*, 8321–8328.
[20] S. Rauschenbach, G. Rinke, R. Gutzler, S. Abb, A. Albarghash, D. Le, T. S. Rahman, M. Durr, L. Harnau, K. Kern, *ACS Nano.* **2017**, *11*, 2420–2427.
[21] J. Laskin, Q. C. Hu, *J. Am. Soc. Mass Spectrom.* **2017**, *28*, 1304–1312.
[22] N. Hauptmann, K. Scheil, T. G. Gopakumar, F. L. Otte, C. Schutt, R. Herges, R. Berndt, *J. Am. Chem. Soc.* **2013**, *135*, 8814–8817.
[23] S. Rauschenbach, G. Rinke, N. Malinowski, R. T. Weitz, R. Dinnebier, N. Thontasen, Z. T. Deng, T. Lutz, P. M. D. A. Rollo, G. Costantini, L. Harnau, K. Kern, *Adv. Mater.* **2012**, *24*, 2761–2767.
[24] V. Franchetti, B. H. Solka, W. E. Baitinger, J. W. Amy, R. G. Cooks, *Int. J. Mass Spectrom. Ion Processes* **1977**, *23*, 29–35.
[25] R. T. Kelly, J. S. Page, I. Marginean, K. Q. Tang, R. D. Smith, *Anal. Chem.* **2008**, *80*, 5660–5665.
[26] S. Pratontep, S. J. Carroll, C. Xirouchaki, M. Streun, R. E. Palmer, *Rev. Sci. Instrum.* **2005**, *76*, 045103.
[27] M. A. Rottgen, K. Judai, J. M. Antonietti, U. Heiz, S. Rauschenbach, K. Kern, *Rev. Sci. Instrum.* **2006**, *77*, 013302.
[28] B. von Issendorff, R. E. Palmer, *Rev. Sci. Instrum.* **1999**, *70*, 4497–4501.
[29] K. D. Gunaratne, V. Prabhakaran, Y. M. Ibrahim, R. V. Norheim, G. E. Johnson, J. Laskin, *Analyst* **2015**, *140*, 2957–2963.
[30] R. E. Palmer, L. Cao, F. Yin, *Rev. Sci. Instrum.* **2016**, *87*, 046103.
[31] A. K. Badu-Tawiah, C. P. Wu, R. G. Cooks, *Anal. Chem.* **2011**, *83*, 2648–2654.
[32] A. K. Badu-Tawiah, J. Cyriac, R. G. Cooks, *J. Am. Soc. Mass Spectrom.* **2012**, *23*, 842–849.
[33] L. Krasny, P. Pompach, M. Strohalm, V. Obsilova, M. Strnadova, P. Novak, M. Volny, *J. Mass Spectrom.* **2012**, *47*, 1294–1302.
[34] A. Y. Li, Q. J. Luo, S. J. Park, R. G. Cooks, *Angew. Chem. Int. Ed.* **2014**, *53*, 3147–3150; *Angew. Chem.* **2014**, *126*, 3211–3214.
[35] A. Y. Li, Z. Baird, S. Bag, D. Sarkar, A. Prabhath, T. Pradeep, R. G. Cooks, *Angew. Chem. Int. Ed.* **2014**, *53*, 12528–12531; *Angew. Chem.* **2014**, *126*, 12736–12739.
[36] V. Prabhakaran, B. L. Mehdi, J. J. Ditto, M. H. Engelhard, B. B. Wang, K. D. D. Gunaratne, D. C. Johnson, N. D. Browning, G. E. Johnson, J. Laskin, *Nat. Commun.* **2016**, *7*, 11399.
[37] P. A. Kottke, J. Y. Lee, A. P. Jonke, C. A. Seneviratne, E. S. Hecht, D. C. Muddiman, M. P. Torres, A. G. Fedorov, *Anal. Chem.* **2017**, *89*, 8981–898.

Manuscript received: June 11, 2018
Version of record online: June 22, 2018